SCATTERING PROPERTIES OF JACKSON CRATER IN THE LUNAR FAR SIDE. Sriram Saran, Anup Das, Shiv Mohan and Manab Chakraborty, Space Applications Centre (ISRO), Ahmedabad, India (saran@sac.isro.gov.in)

Introduction: Large and fresh lunar craters are best targets to understand impact cratering, because space weathering and subsequent small impacts are the major processes that disturb the original structure of ejecta units over time [1]. Analysis of morphology and ejecta distribution of such fresh craters can give important clues to reconstruct the impact event and pre-impact sub surface structures. To illustrate this, scattering properties of Jackson crater (70 km-diameter), one of the most enigmatic features in the northern hemisphere of lunar far side, have been analysed in this study. Bright rays streak for hundreds of kilometres across the lunar surface originate from Jackson crater, which has a large forbidden zone in the NW sector suggesting that Jackson was formed by an oblique impact along the NW-SE direction [1]. The analysis was carried out using Chandrayaan-1 Mini-SAR data supported by high resolution optical datasets from Lunar Reconnaissance Orbiter Camera (LROC) Narrow Angle Camera (NAC) on the Lunar Reconnaissance Orbiter (LRO).

Background: Mini-SAR was an S-band (2.38GHz) hybrid-circular polarimetric imaging radar [2] flown on ISRO's Chandrayaan-1 mission in October 2008. It transmitted in left circular polarizations (LCP) and coherently received the returned signals in H and V polarizations. It has imaged the lunar surface at 35° incident angle with a ground range resolution of 150m [3]. This configuration allows for the calculation of Stokes parameters that are used to produce useful products such as the circular polarization ratio (CPR) and the degree of linear polarization. The radar data collected can provide a wealth of additional information about the lunar surface, such as surface roughness, dielectric properties, and topography [4]. Properties such as roughness may not be as obvious in the visible or infrared image data, so radar datasets are complementary to them. Further, the relatively large penetration depth of the radar (several meters) allows for sampling of the near subsurface [5].

Data and method: For this study, along with the total backscattered power S_0, another relevant daughter product CPR, defined as

$$CPR = (S_0 - S_3) / (S_0 + S_3) \qquad (1)$$

where S_0 and S_3 represent the first and fourth elements of Stokes vector respectively, has been taken into use. Variations in radar backscatter along with CPR serve as quantitative estimates of surface roughness and surface composition and are very useful for differentiating independent geologic deposits [6]. Also, the decomposition of m-δ ($m = (S_1^2 + S_2^2 + S_3^2)^{1/2}/S_0$ - degree of polarization; $\delta = \tan^{-1}(-S_3/S_2)$ - relative phase between two polarization channels) feature space [2] has been implemented in this study which provides the dominant scattering mechanism corresponding to a target or within a radar resolution cell, expressed as

$$\left.\begin{aligned} \boldsymbol{R} &= \sqrt{S_0 \times m \times (1+\sin\delta)/2} \\ \boldsymbol{G} &= \sqrt{S_0 \times (1-m)} \\ \boldsymbol{B} &= \sqrt{S_0 \times m \times (1-\sin\delta)/2} \end{aligned}\right\} \qquad (2)$$

where, the total power $S_0 = R^2+B^2+G^2$ and R, G, B represent double-bounce, volume and single bounce backscatter, respectively. The LROC NAC cameras on LRO are a pair of monochrome line scan imagers that acquire data at resolutions up to 0.5 m [7]. The NAC optical images were used to characterize the distribution of radar scatterers that are observed in Mini-SAR CPR data in order to understand how variations in such distributions affect CPR.

Discussion: Using Mini-SAR data along with the corresponding high resolution optical data from the NAC (LROC), interior deposits and unique ejecta deposits associated with large, fresh craters can be examined to understand the impact cratering process.

Crater walls. Variations in radar backscatter and CPR values can serve as an indicator of topographic variability, which is related to the local slopes of the terrain with respect to the radar look direction. The crater walls of Jackson are slumped with a number of terraces that step downwards into the crater's interior as observed in the Mini-SAR S_0 image (Fig. 1a) and corresponding LRO NAC image (Fig. 2). This complex topography associated with the walls of the crater lead to enhanced backscatter, thereby a decline in CPR values (Fig. 1b) due to high OC (Opposite sense Circular) returns. Also, there is a significant contribution of double bounce scattering from the crater walls as seen from the decomposition image (Fig. 1c). This arises from the conditions where the inner walls or the rock surfaces form the proper double-bounce geometry.

Interior deposits. Young, fresh craters are distinctive in radar images obtained with the Mini-SAR. Because of the surface roughness associated with Jackson crater's interior, it is characterized by very high backscatter and CPR values ranging from 0.7 to 2.4 (Fig. 1b). These high values are due to sensitivity of the 12.6-cm wavelength radar to few-centimeter and larger scale radar scatterers like boulders, formed due to gradual cooling of post-impact melt material. It can be observed that the dominant scattering mechanism is volume scattering at the crater's interior, as seen in Fig. 1c. This implies that the crater floor is very rough to the incident radar signal and hence less energy penetrates into the regolith layer. Therefore, scattering contribution from the buried rocks and surface-volume interaction decreases significantly.

Ejecta deposits. Along with abundant few-cm scale surface rocks, the ejecta deposits surrounding Jackson crater consist of a heterogeneous distribution of impact melt ponds [1] which can be observed in the corresponding high resolution NAC image (Fig.2). As the melt ponds are smooth surfaces, they are seen as dark patches in the radar image concentrated at both top and bottom of the crater walls characterized by very low backscatter. On the contrary, due to the presence of excessive rock population, very bright patches can be observed at the extreme Northern and Southern ends of the crater walls with enhanced backscatter values.

Summary: The Mini-SAR instrument on the Chandrayaan-1 orbiter provided important data regarding the surface roughness, topography, and dielectric properties of the lunar surface. The information gained from this data provides a unique perspective in understanding the evolution of the lunar surface. Using Mini-SAR data supported with high resolution optical imagery like the NAC instrument onboard LRO, characterization of floor and the distribution of ejecta deposits of large fresh lunar craters has been attempted. This work helps in understanding the terrain characteristics of the lunar far side using radar data which is not possible from Earth based observations. It will also lead, more generally, to a better understanding of the cratering process. Future work will include studying more data for different terrains around the Moon, along with new high resolution optical imagery, and correlating them with estimates of surface roughness and mineral maps derived optically.

References: [1] Hirata N. et al. (2010) *LPS XLI*, Abstract #1585. [2] Raney R. K. (2007) *IEEE Trans. Geosci. Remote Sens.*, *45*, 3397-3404. [3] Spudis P. D. et al. (2010) *Geophys. Res. Letters*, *37*, L06204. [4] Patterson G. W. et al. (2010) *LPS XLI*, Abstract #2316. [5] Campbell B. A. et al. (2010) *Icarus*, 208, 565-573. [6] Payne C. J. et al. (2010) *LPS XLI*, Abstract #1211. [7] Robinson et al. (2007), *Space Sci. Rev.*, 150, doi: 10.1007/s11214-010-9634-2.

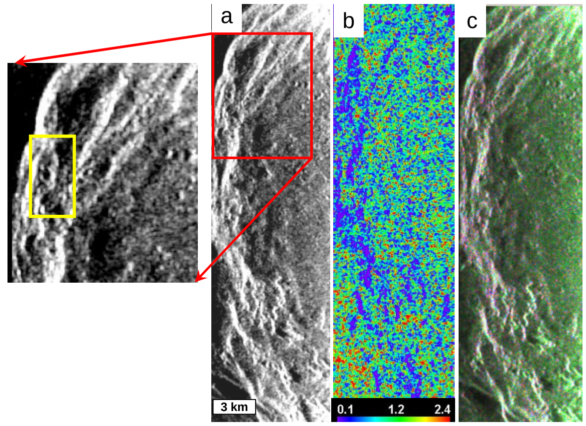

Figure 1 Jackson crater as seen by Mini-SAR in (a) S_0 (b) CPR and (c) m-δ decomposition images. Decomposition image represents Double bounce (Red), Volume (Green) and Surface (Blue) scattering contributions**.**

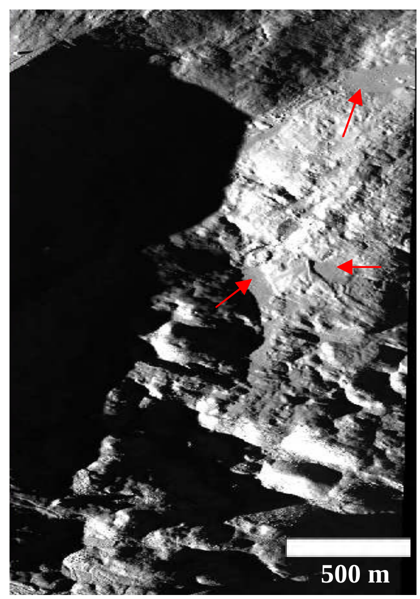

Figure 2 Close-up view of LRO NAC image (incidence angle of 68°) showing the slumped wall-portion of Jackson crater as outlined in yellow box in fig 1a. Melt ponds are indicated by arrows. The image has a resolution of 1.41m.